ICOSSAR 2021
The 13th International Conference on Structural Safety and Reliability (ICOSSAR 2021), June 21-25, 2021, Shanghai, P.R. China
J. Li, Pol D. Spanos, J.B. Chen & Y.B. Peng (Eds)

A p-refined Multilevel quasi-Monte Carlo method with Supermesh Construction applied to a Geotechnical Slope Stability Problem

Philippe Blondeel[a], Pieterjan Robbe[a], Stijn François[b], Geert Lombaert[b], and Stefan Vandewalle[a]

[a] *Dep. Computer Science, KU Leuven, Belgium, E-mail: {philippe.blondeel,pieterjan.robbe,stefan.vandewalle}@kuleuven.be.*
[b] *Dep. Civil Engineering, KU Leuven, Belgium, E-mail: {stijn.francois,geert.lombaert}@kuleuven.*

ABSTRACT: Problems in civil engineering are often characterized by significant uncertainty in their material parameters. Sampling methods are a straightforward manner to account for this uncertainty, which is typically modeled as a random field. The underlying engineering problem is typically discretized by means of the Finite Element (FE) method. Adequately incorporating the uncertainty in the FE model is paramount when performing stochastic simulations. In this work, we present two novel approaches to incorporate this uncertainty when considering the p-refined Multilevel quasi-Monte Carlo method (p-MLQMC) as a stochastic method. The p-MLQMC method is a recently proposed improved Multilevel Monte Carlo method which combines a hierarchy of p-refined FE meshes with a quasi-Monte Carlo sampling rule based on rank-1 lattice sequences. We show that the two new approaches, the 'Supermesh Global Approach' (SGA) and the 'Supermesh Local Approach' (SLA) outperform our previously proposed approaches in terms of computational cost. Furthermore, we also compare in terms of computational cost, SGA and SLA against the existing Multilevel (quasi)-Monte Carlo methods (h-ML(Q)MC) which are based on an h-refinement scheme.

1 INTRODUCTION

Problems in the engineering sciences are typically subject to uncertainty. This uncertainty can be present in the material parameters, as for example, the cohesion of the soil in a slope stability problem. Purely deterministic solutions provide only limited insight into the assessment of structural safety or stability, under uncertain material conditions. There is therefore an increasing need for fast stochastic methods which can assess the uncertainty on the output of a model. A popular stochastic sampling method is the Multilevel Monte Carlo Method (MLMC). First developed by Giles, see Giles (2015, 2008), the MLMC methods relies on a hierarchy of meshes with increasing resolution, also known as *levels*, in order to reduce the total computational cost. In the MLMC method, most of the samples are taken on low-resolution and computationally cheap meshes, while a decreasing number of samples are taken on high-resolution and computationally expensive meshes. The efficiency of the MLMC method is determined by the correlation between the subsequent resolution levels. A high correlation results in a more efficient method. The mesh hierarchy is typically constructed by selecting a coarse Finite Element (FE) mesh approximation of the considered problem, and recursively applying the h-refinement scheme. While MLMC outperforms standard Monte Carlo (MC) in terms of computational cost by at least a factor 10 for problems in civil engineering, see Blondeel et al. (2018), many improvements upon MLMC have been devel-

oped. One notable improvement is the Multilevel quasi-Monte Carlo method, see Giles and Waterhouse (2009). Here, the randomly generated Monte Carlo sample points are replaced with deterministically generated quasi-Monte Carlo (QMC) sample points. Using this approach, we have demonstrated that the MLQMC method outperforms the MLMC method in terms of computational cost, see Blondeel et al. (2019). However, because of the type of mesh refinement used for classical Multilevel (quasi-)Monte Carlo (h-ML(Q)MC), i.e., h-refinement, the computational cost, which is necessary to compute one sample on a high-resolution mesh, is high. This stems from a geometrical increase of the number of degree of freedom (DOF) for each refined mesh, which results in a high number of DOF's on the higher resolution meshes, and thus a high cost to compute one solve on these meshes. This led us to develop a novel multilevel method, called p-refined Multilevel quasi-Monte Carlo (p-MLQMC), see Blondeel et al. (2020). This multilevel method combines a mesh hierarchy based on a p-refinement scheme with a QMC sampling rule. This approach yields significant computational cost savings with respect to h-MLMC. However, incorporating the uncertainty in the FE model presents more of a challenge when the p-MLQMC method is used than when the h-MLMC method is used. We therefore have investigated how to adequately incorporate the uncertainty, modeled as a random field by means of the Karhunen–Loève expansion, in the FE model, see Blondeel et al. (2021). In the context of incorporating the uncertainty when using the p-MLQMC method, we distinguished different approaches, all based on the integration point method, see Matthies et al. (1997). The two main approaches are the Non-Nested Approach (NNA), and the Local Nested Approach (LNA). The core idea unifying these methods is to account for the discrete random field samples, obtained by the evaluation of the random field at certain carefully chosen evaluation points, during the numerical integration of the element stiffness matrices. The choice of the random field evaluation points is crucial in order to obtain a high correlation between the different levels, and so to achieve a corresponding low computational cost. The correlation directly impacts the variance reduction over the levels, i.e., the decrease of the variance of the differences of a quantity of interest with increasing level, determines the number of samples per level. In this work we present two improved methods, which are also based on the integration point method. These methods are the Supermesh Global Approach (SGA) and the Supermesh Local Approach (SLA). The model problem on which we benchmark these approaches consists of a slope stability problem. The slope stability problem is a geotechnical engineering problem, where the goal is to assess the stability of natural or man-made slopes. This stability can, among others, be assessed by investigating the vertical displacement of the top of the slope.

The paper is structured as follows. First we introduce the concepts behind p-MLQMC. Second we discuss how the uncertainty is modeled and how it needs to be account for, in the FE model. Third we discuss the underlying FE solver, and present the model problem. Fourth we present the results comparing the previous approaches (NNA, LNA) with the newly proposed ones (SGA, SLA). Last we compare the computational costs of SGA and SLA against h-ML(Q)MC for a given set of tolerances.

2 MULTILEVEL METHODS

The expected value of a function P against an s-dimensional probability density function ϕ is defined by

$$\mathbb{E}[P] := \int_{\mathbb{R}} \cdots \int_{\mathbb{R}} P(x_1,\ldots,x_s)\,\phi(x_1,\ldots,x_s)\,\mathrm{d}x_1 \cdots \mathrm{d}x_s = \int_{\mathbb{R}^s} P(\boldsymbol{x})\,\phi(\boldsymbol{x})\,\mathrm{d}\boldsymbol{x}. \tag{1}$$

In order to approximate the integral in Eq. (1), an equal-weight quadrature rule can be used. An example of such an equal-weight quadrature rule is the Monte Carlo method. In our

case, the function P is obtained by means of a FE method on a chosen discretization level L, i.e., $\mathbb{E}[P] \approx \mathbb{E}[P_{\mathrm{L}}]$. This introduces a first approximation error. The integral itself is then approximated using a quadrature rule, i.e., $\mathbb{E}[P_{\mathrm{L}}] \approx Q_{\mathrm{L}}^{\mathrm{MLQMC}}$. This introduces a second approximation error.

2.1 *Telescoping Sum and Mesh Hierarchies*

The core idea of Multilevel Monte Carlo methods is to rely on a hierarchy of meshes in order to achieve a speedup with respect to Monte Carlo. The expected value of a quantity of interest on a high-resolution mesh is written as the expected value of a quantity of interest on a low-resolution mesh to which a series of correction terms are added. In particular, given a hierarchy of approximations $P_0, P_1, \ldots, P_{\mathrm{L}}$ for the quantity of interest P computed on an increasingly higher resolution mesh, we have the telescopic sum identity

$$\mathbb{E}[P_{\mathrm{L}}] = \mathbb{E}[P_0] + \sum_{\ell=1}^{\mathrm{L}} \mathbb{E}[P_\ell - P_{\ell-1}]. \tag{2}$$

The speedup is then achieved by taking a majority of samples on low-resolution and computationally cheap meshes, and by taking only a decreasing number of samples on higher resolution and computationally expensive meshes. Classically, the hierarchy of meshes is obtained by applying an h-refinement scheme to a low-resolution mesh model. However, here we opt for a hierarchy based on a p-refinement scheme, i.e., increasing the polynomial's order of the shape functions with increasing level. In Figure 1, we show the first two levels of the hierarchy. Here, the FE nodal points are represented as black dots. A more thorough discussion of the slope stability problem and the FE model is given in §4.

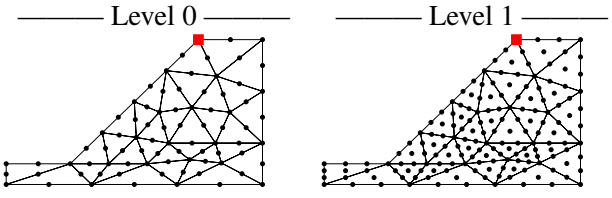

Figure 1. p-refined hierarchy of meshes used for the slope stability problem with the QoI indicated by ■.

2.2 *Estimators and Variances*

The MLQMC estimator used in the p-MLQMC method is given by

$$Q_{\mathrm{L}}^{\mathrm{MLQMC}} := \frac{1}{R_0}\sum_{r=1}^{R_0}\frac{1}{N_0}\sum_{n=1}^{N_0} P_0(\mathbf{u}_0^{(r,n)}) + \sum_{\ell=1}^{\mathrm{L}}\frac{1}{R_\ell}\sum_{r=1}^{R_\ell}\left\{\frac{1}{N_\ell}\sum_{n=1}^{N_\ell}\left(P_\ell(\mathbf{u}_\ell^{(r,n)}) - P_{\ell-1}(\mathbf{u}_\ell^{(r,n)})\right)\right\}. \tag{3}$$

Using the short-hand notation $\Delta P_\ell := P_\ell - P_{\ell-1}$ with $P_{-1} := 0$, the MLQMC estimator can be written as

$$Q_{\mathrm{L}}^{\mathrm{MLQMC}} = \sum_{\ell=0}^{\mathrm{L}}\frac{1}{R_\ell}\sum_{r=1}^{R_\ell}\frac{1}{N_\ell}\sum_{n=1}^{N_\ell}\Delta P_\ell(\mathbf{u}_\ell^{(r,n)}) \tag{4}$$

$$=: \sum_{\ell=0}^{\mathrm{L}}\Delta Q_\ell, \tag{5}$$

where ΔQ_ℓ is an estimator for the difference ΔP_ℓ. It is important to note that we assume that the sample points $\mathbf{u}_\ell^{(r,n)}$ are independent of r. More details on the construction of the sample points will be given in the next subsection.

The MLQMC estimator is an unbiased estimator for $\mathbb{E}[P_{\mathrm{L}}]$, since

$$\mathbb{E}\left[Q_{\mathrm{L}}^{\mathrm{MLQMC}}\right] = \mathbb{E}[P_{\mathrm{L}}]. \tag{6}$$

Its variance is given by

$$\mathbb{V}\left[Q_{\mathrm{L}}^{\mathrm{MLQMC}}\right] = \sum_{\ell=0}^{\mathrm{L}}\mathbb{V}\left[\Delta Q_\ell^{\mathrm{MLQMC}}\right], \tag{7}$$

where the variance $\mathbb{V}[\Delta Q_\ell]$ can be approximated by the sample variance $\mathcal{V}_\ell$ over the R_ℓ independent contributions, i.e.,

$$\mathcal{V}_\ell := \frac{1}{R_\ell(R_\ell-1)}\sum_{r=1}^{R_\ell}\left(\frac{1}{N_\ell}\sum_{n=1}^{N_\ell}\Delta P_\ell^{(r,n)} - \Delta Q_\ell\right)^2. \tag{8}$$

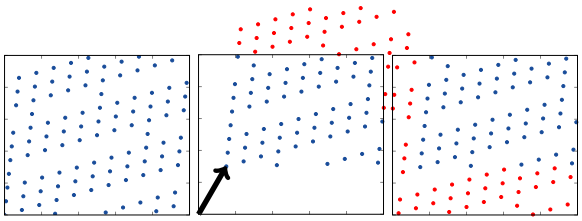

Figure 2. Illustrative example of the random shifting procedure applied to points belonging to a rank-1 lattice sequence.

2.3 *On the choice of the sample points* $\mathbf{u}^{(r,n)}$

While the MLMC method is based on (pseudo-)random distributed sample points, the MQLMC method uses deterministic sample points, i.e., QMC points, $\mathbf{u}_\ell^{(r,n)}$. More specifically, here we use a rank-1 lattice sequence. In order to recover unbiased estimates of the estimator, the computation of the estimator and its variance include an averaging over a number of shifts $r = 1, 2, ..., R_\ell$ on each level ℓ. The procedure of random shifting consists of adding to each point of the lattice sequence, a uniformly distributed number $\Xi_r \in [0,1)^s$ after which the fractional part is taken. This is illustrated in Figure 2. In our implementation $R_\ell = 10$ for $\ell = \{0, \ldots, \mathrm{L}\}$.

The shifted version of the lattice points is given by

$$\mathbf{u}^{(r,n)} := \Phi^{-1}\left(\mathrm{frac}\left(\phi_2(n)\mathbf{z} + \Xi_r\right)\right), n \in \mathbb{N}, \tag{9}$$

where Φ^{-1} is the inverse cumulative density function (CDF) of the distribution of interest, $\mathrm{frac}(x) := x - \lfloor x \rfloor, x > 0$, ϕ_2 is the radical inverse function in base 2 and $\mathbf{z}$ is an s-dimensional vector of positive integers. The generating vector $\mathbf{z}$ was constructed with the component-by-component (CBC) algorithm with decreasing weights, $\gamma_j = 1/j^2$, see Kuo (2007). In this paper, we consider a standard normal distribution.

2.4 *Variance Reduction*

Multilevel methods rely on a variance reduction across the levels in order to achieve a computational speedup. This means that the sample variance of the difference for increasing level ℓ continuously decreases, i.e., $\mathbb{V}[\Delta P_1] > \mathbb{V}[\Delta P_2] > \cdots > \mathbb{V}[\Delta P_\mathrm{L}]$. This variance reduction is only obtained when a strong positive correlation is achieved between the results of two successive levels, i.e.,

$$\begin{aligned}\mathbb{V}[\Delta P_\ell] &= \mathbb{V}[P_\ell - P_{\ell-1}] \\ &= \mathbb{V}[P_\ell] + \mathbb{V}[P_{\ell-1}] - 2\mathrm{cov}(P_\ell, P_{\ell-1}),\end{aligned} \tag{10}$$

where $\mathrm{cov}(P_\ell, P_{\ell-1}) = \rho_{\ell,\ell-1}\sqrt{\mathbb{V}[P_\ell]\mathbb{V}[P_{\ell-1}]}$ is the covariance between P_ℓ and $P_{\ell-1}$ with $\rho_{\ell,\ell-1}$ the correlation coefficient. The value of $\mathrm{cov}(P_\ell, P_{\ell-1})$ must be large in order to have a large variance reduction, and hence an efficient multilevel method.

2.5 *Number of Samples per Level*

In the MLQMC method, the number of samples is computed by means of a 'doubling' algorithm. The procedure starts by computing a number of warm-up samples together with a user-defined number of shifts on each level. From these samples $\mathbb{V}\left[\Delta Q_\ell^{\mathrm{MLQMC}}\right]$ is estimated on each level ℓ, see Eq. (8). The iterative step consists of selecting the level τ on which the ratio of the variance of the estimator with the sample cost is maximal, i.e., $\underset{\tau\in\mathrm{L}}{\mathrm{argmax}}\,(\mathcal{V}_\tau/C_\tau)$. On this level τ the number of samples is multiplied with a constant factor. This procedure is repeated until $\mathbb{V}\left[Q_\mathrm{L}^{\mathrm{MLQMC}}\right] < \frac{\varepsilon^2}{2}$. In our approach, this constant is chosen as 1.2.

3 REPRESENTING THE UNCERTAINTY

In the slope stability problem, the cohesion of the soil is uncertain. This uncertainty is modeled as a random field, which is constructed by means of the Karhunen–Loève (KL) expansion,

$$Z(\mathbf{x}, \omega) = \overline{Z}(\mathbf{x}) + \sum_{n=1}^{s} \sqrt{\theta_n}\xi_n(\omega)b_n(\mathbf{x}). \tag{11}$$

Here, $\overline{Z}(\mathbf{x})$ is the mean of the field and $\xi_n(\omega)$ denote i.i.d. standard normal random variables. The symbols θ_n and $b_n(\mathbf{x})$ denote the eigenvalues and eigenfunctions respectively, which are the solutions of the eigenvalue problem $\int_D C(\mathbf{x},\mathbf{y})b_n(\mathbf{y})\mathrm{d}\mathbf{y} = \theta_n b_n(\mathbf{x})$ with a given covariance kernel $C(\mathbf{x},\mathbf{y})$. Note that in order to represent the uncertainty of the cohesion of the soil, we do not use $Z(\mathbf{x},\omega)$ but $\exp(Z(\mathbf{x},\omega))$, see §4.

3.1 *Incorporation into the model*

In order to incorporate the uncertainty in the FE model with the p-MLQMC method, we use the integration point method, see Matthies et al. (1997). Within the framework of the integration point method, we compute discrete instances of the random field, using Eq. (11), evaluated at the points $\mathbf{x} = \{\mathrm{x}^{(i)}\}_{i=1}^n$. The goal thus consists of finding 'adequate' points $\mathbf{x}$ where to evaluate the random field.

In the integration point method, we incorporate the uncertainty at the level of the FE stiff-

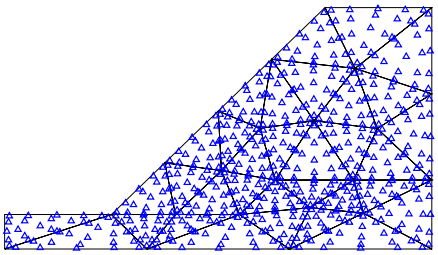

Figure 3. Slope stability mesh with quadrature points in global coordinates designated by △.

ness matrices. The assembly of the FE stiffness matrices results in the global stiffness matrix $\mathbf{K}$, see § 4. Practically, the FE stiffness matrices are obtained by means of numerical integration where we use a set of quadrature points $\mathbf{q} = \{\mathrm{q}^{(i)}\}_{i=1}^{n}$, i.e.,

$$\mathbf{K^e} = \int_{\Omega_e} \mathbf{B}^T \mathbf{D}\mathbf{B} d\Omega_e \approx \sum_{i=1}^{n} \mathrm{w}^{(i)} (\mathbf{B}^{(i)})^T \mathbf{D}^{(i)} \mathbf{B}^{(i)}, \tag{12}$$

where the matrix $\mathbf{B}^{(i)} = \mathbf{B}(\mathrm{q}^{(i)})$ contains the derivatives of the shape functions, evaluated at the quadrature points $\mathrm{q}^{(i)}$, the matrix $\mathbf{D}^{(i)} = \mathbf{D}\left(\mathrm{x}^{(i)}, \cdot\right)$ contains the model uncertainty evaluated at point $\mathrm{x}^{(i)}$, and $\mathrm{w}^{(i)}$ is a quadrature weight. The uncertainty in the matrix $\mathbf{D}^{(i)}$ originates from the evaluation of the random field at a carefully chosen spatial location $\mathrm{x}^{(i)}$. An example of the slope stability mesh containing the location of all the quadrature points in global (mesh) coordinates is shown in Figure 3.

In previous work, see Blondeel et al. (2021, 2020), we presented different possible implementations of the integration point method. We constructed for each level ℓ a set of points $\mathbf{x}_\ell := \{\mathrm{x}_\ell^{(i)}\}_{i=1}^{n_\ell}$, where the random field was evaluated. The resulting discrete random field sample points were afterwards taken into account during numerical integration of Eq. (12). Note that the number of evaluation points of the random field increases with increasing level, i.e., $n_0 < n_1 < \ldots < n_\mathrm{L}$. We highlight the two most important approaches from our previous work, the Non-Nested Approach (NNA) and the Local Nested Approach (LNA). In the NNA method, the random field is evaluated in the quadrature points, i.e., $\mathrm{x}_\ell^{(i)} = \mathrm{q}_\ell^{(i)}$ for $i = 1, 2, \ldots, n$. In the LNA method, to compute the difference ΔP_ℓ on level ℓ, the random field is evaluated in the n_ℓ quadrature points $\mathbf{q}_\ell$ for the evaluation of P_ℓ, and in the $n_{\ell-1}$ *closest* quadrature points of $\mathbf{q}_\ell$ for the evaluation of $P_{\ell-1}$. LNA showed a speedup up to a factor 5 with respect to NNA, by providing a stronger correlation between the solutions of two successive levels, see §2.4. However, LNA suffered from a major drawback, an additional bias was introduced in the computed expected value obtained by evaluating the telescopic sum in Eq. (2). In the next section, we present two improved approaches, which do not suffer from this additional bias, but still provide a strong correlation between the solution of two successive levels.

3.1.1 *Supermesh Global Approach*

Suppose we have a set of quadrature points $\mathbf{q}_\ell = \{\mathrm{q}_\ell^{(i)}\}_{n=1}^{n_\ell}$ available on each level $\ell = 0, 1, \ldots, \mathrm{L}$. In the Supermesh Global approach (SGA), all the quadrature points on each level are mapped to one Supermesh. This Supermesh then contains all the quadrature points of all the levels, i.e., $\mathbf{q}_\mathrm{supermesh} := \cup_{\ell=0}^{\mathrm{L}} \mathbf{q}_\ell$. This is illustrated in Figure 4 on one reference triangular element. The quadrature points $\mathbf{q}_\ell$ on the different levels are represented by △. The evaluation points, represented by ●, used for the Karhunen–Loève expansion are then equal to $\mathbf{q}_\mathrm{supermesh}$, i.e., $\mathbf{x}_\mathrm{supermesh} := \mathbf{q}_\mathrm{supermesh}$. In Algorithm 1 we present, in pseudocode, the procedure used to obtain the required samples $\mathbf{Z}_\ell$ and $\mathbf{Z}_{\ell-1}$ from the Gaussian random field, evaluated in $\mathbf{q}_\ell$ (respectively, $\mathbf{q}_{\ell-1}$), i.e., $\mathbf{Z}_\ell := Z(\mathbf{x}_\ell, \cdot)$ and $\mathbf{Z}_{\ell-1} := Z(\mathbf{x}_{\ell-1}, \cdot)$, when computing a sample from the multilevel difference ΔP_ℓ.

We thus only compute instances of $Z(\mathbf{q}_\mathrm{supermesh}, \cdot)$. The values for $\mathbf{Z}_\ell$ and $\mathbf{Z}_{\ell-1}$ are restricted from $Z(\mathbf{q}_\mathrm{supermesh})$. The restricted random field is then taken into account during the numerical integration of the element stiffness matrices, see Eq. (12).

In the case of SGA, no bias is present on the computed expected value obtained by means of evaluating the telescoping sum property. This is because the approximations, ΔP_ℓ, on the different levels ℓ all have the same stochastic

ICOSSAR 2021
The 13th International Conference on Structural Safety and Reliability (ICOSSAR 2021), June 21-25, 2021, Shanghai, P.R. China
J. Li, Pol D. Spanos, J.B. Chen & Y.B. Peng (Eds)

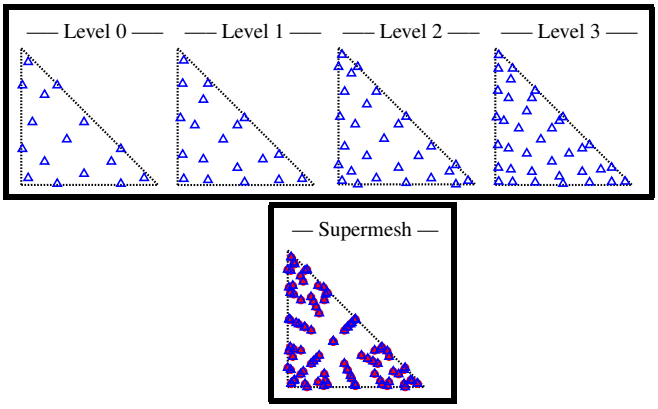

Figure 4. Illustration of the Supermesh Global Approach.

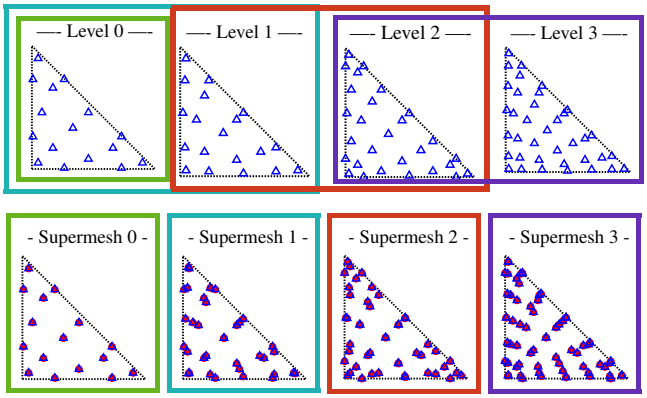

Figure 5. Illustration of the Supermesh Local Approach.

Data: current level ℓ;
quadrature points $\mathbf{q}_\ell$ with $\ell = 0,\ldots,\mathrm{L}$;
Result: sample of the random field $\mathbf{Z}_\ell$ on level ℓ;
sample of the random field $\mathbf{Z}_{\ell-1}$ on level $\ell-1$ if $\ell > 0$;
$\mathbf{q}_{\text{supermesh}} \leftarrow \bigcup_{\ell=0}^{\mathrm{L}} \mathbf{q}_\ell$;
$\mathbf{Z}_{\text{supermesh}} \leftarrow Z(\mathbf{q}_{\text{supermesh}}, \cdot)$;
$\mathbf{Z}_\ell \leftarrow \mathbf{Z}_{\text{supermesh}}|_{\mathbf{q}^{(i)}_{\text{supermesh}} \in \mathbf{q}_\ell}$;
if $\ell > 0$ **then**
  $\mathbf{Z}_{\ell-1} \leftarrow \mathbf{Z}_{\text{supermesh}}|_{\mathbf{q}^{(i)}_{\text{supermesh}} \in \mathbf{q}_{\ell-1}}$;
end

Algorithm 1. Computing the required samples of the Gaussian random field for the evaluation of the multilevel difference ΔP_ℓ using SGA.

properties, i.e., all random field instances are restricted from the random field computed on the supermesh. However, the level extensibility is not present in this approach. If an additional level is needed by the multilevel simulation, a new supermesh needs to be generated, with the addition that the previously computed samples cannot be reused in the new mesh hierarchy.

3.1.2 *Supermesh Local Approach*

Because there was no level extensibility present in SGA, we developed an approach where the level extensibility is present, i.e., the Supermesh Local Approach (SLA). The selection of random field evaluation points in SLA is similar to the one in the Supermesh Global Approach (SGA), except we do not construct one "big" supermesh, but construct multiple "smaller" supermeshes on each level $\ell = 0,\ldots,\mathrm{L}$, i.e., for every set of consecutive levels, we construct one supermesh. The procedure is as follows. For all levels $\ell = 0,\ldots,\mathrm{L}$ we compute $\mathbf{q}_{\ell,\text{supermesh}}$ such that $\mathbf{q}_{\ell,\text{supermesh}} := \mathbf{q}_\ell \cup \mathbf{q}_{\ell-1}$ with $\mathbf{q}_{-1} := \varnothing$, and evaluate the random field $\mathbf{Z}_{\ell,\text{supermesh}}$ in all points $\mathbf{q}_{\ell,\text{supermesh}}$. Next, the values for $\mathbf{Z}_\ell$ and $\mathbf{Z}_{\ell-1}$ are obtained by restriction of $\mathbf{Z}_{\ell,\text{supermesh}}$, see Algorithm 2. The approach is also illustrated in Figure 5, by means of colored frames.

Data: current level ℓ;
quadrature points $\mathbf{q}_\ell$ with $\ell = 0,\ldots,\mathrm{L}$ and $\mathbf{q}_{\ell-1} = \varnothing$;
Result: sample of the random field $\mathbf{Z}_\ell$ on level ℓ;
sample of the random field $\mathbf{Z}_{\ell-1}$ on level $\ell-1$ if $\ell > 0$;
$\mathbf{q}_{\ell,\text{supermesh}} \leftarrow \mathbf{q}_\ell \cup \mathbf{q}_{\ell-1}$;
$\mathbf{Z}_{\ell,\text{supermesh}} \leftarrow Z(\mathbf{q}_{\ell,\text{supermesh}}, \cdot)$;
$\mathbf{Z}_\ell \leftarrow \mathbf{Z}_{\ell,\text{supermesh}}|_{\mathbf{q}^{(i)}_{\ell,\text{supermesh}} \in \mathbf{q}_\ell}$;
if $\ell > 0$ **then**
  $\mathbf{Z}_{\ell-1} \leftarrow \mathbf{Z}_{\ell,\text{supermesh}}|_{\mathbf{q}^{(i)}_{\ell,\text{supermesh}} \in \mathbf{q}_{\ell-1}}$;
end

Algorithm 2. Computing the required samples of the Gaussian random field for the evaluation of the multilevel difference ΔP_ℓ using SLA.

This procedure implies that in the evaluation of the multilevel differences, the different realizations of the Gaussian random field with the same quadrature points $\mathbf{q}_\ell$ may originate from different supermeshes. For example, when computing a sample of ΔP_τ, and a sample of $\Delta P_{\tau-1}$, two supermeshes are involved: one with $n_{\tau,\text{supermesh}} := |\mathbf{q}_\tau| + |\mathbf{q}_{\tau-1}|$ with quadrature points $\mathbf{q}_{\tau,\text{supermesh}} := \mathbf{q}_\tau \cup \mathbf{q}_{\tau-1}$ for the evaluation of ΔP_τ and one with $n_{\tau-1,\text{supermesh}} := |\mathbf{q}_{\tau-1}| + |\mathbf{q}_{\tau-2}|$ with quadrature points $\mathbf{q}_{\tau-1,\text{supermesh}} := \mathbf{q}_{\tau-1} \cup \mathbf{q}_{\tau-2}$ for the evaluation of $\Delta P_{\tau-1}$. The Gaussian random field $\mathbf{Z}_{\tau-1}$ will then be computed from the supermesh with $n_{\tau,\text{supermesh}}$ points for the evaluation of ΔP_τ, and from the supermesh

ICOSSAR 2021
The 13th International Conference on Structural Safety and Reliability (ICOSSAR 2021), June 21-25, 2021, Shanghai, P.R. China
J. Li, Pol D. Spanos, J.B. Chen & Y.B. Peng (Eds)

with $n_{\tau-1,\text{supermesh}}$ points for the evaluation of $\Delta P_{\tau-1}$.

Contrary to the case of SGA, in case of SLA an infinitesimal bias is present on the computed expected value obtained by means of evaluating the telescoping sum property. As was stated above, the approximations ΔP_τ and $\Delta P_{\tau-1}$, are computed from random field samples generated on different supermeshes, i.e., $\mathbf{Z}_{\tau,\text{supermesh}}$ and $\mathbf{Z}_{\tau-1,\text{supermesh}}$. For the computation of $\mathbf{Z}_{\tau,\text{supermesh}}$, the set of quadrature points $\mathbf{q}_{\tau,\text{supermesh}} := \mathbf{q}_\tau \cup \mathbf{q}_{\tau-1}$ is used, while for $\mathbf{Z}_{\tau-1,\text{supermesh}}$, the set of quadrature points $\mathbf{q}_{\tau-1,\text{supermesh}} := \mathbf{q}_{\tau-1} \cup \mathbf{q}_{\tau-2}$ is used. The supermeshes share in part the same quadrature points, i.e., $\mathbf{q}_{\tau-1}$, this ensures that both supermeshes exhibit the same stochastic properties. However, we observe that the numerically computed eigenvalues and eigenvector of the Karhunen–Loève expansion, see Eq. (11), differ slightly for both supermeshes. This is because $\mathbf{Z}_{\tau-1,\text{supermesh}}$ is not computed in $\mathbf{q}_\tau$, and $\mathbf{Z}_{\tau,\text{supermesh}}$ is not computed in $\mathbf{q}_{\tau-2}$. This will lead to an infinitesimal bias being present on the computed expected value obtained by means of the telescoping sum. Contrary to SGA, in SLA the mesh hierarchy is easily extensible. Additional level can easily be added while reusing the computed samples from the previous mesh hierarchy.

3.2 *Computational Cost Discussion*

In this section we briefly discuss the off-line cost for SGA and SLA. This off-line cost is the cost of computing the eigenvalues and eigenvectors used in the Karhunen–Loève expansion. This cost is proportional to $O(n^3)$, where n stands for the discrete number of points in which the eigenvalues and eigenvectors are computed. For SGA, the total computational cost is proportional to the number of points in the union of all the quadrature points, i.e., $O\left(\left|\cup_{\ell=0}^{\mathrm{L}} \mathbf{q}_\ell\right|^3\right)$, where $|\cdot|$ stands for the cardinality operator. We know that $\left|\cup_{\ell=0}^{\mathrm{L}} \mathbf{q}_\ell\right| \leq \cup_{\ell=0}^{\mathrm{L}} |\mathbf{q}_\ell| \leq \sum_{\ell=0}^{L} n_\ell$, implying that $O\left(\left|\cup_{\ell=0}^{\mathrm{L}} \mathbf{q}_\ell\right|^3\right) \leq O\left(\left(\sum_{\ell=0}^{L} n_\ell\right)^3\right)$. For SLA, the computational cost is proportional to $O\left(\sum_{\ell=1}^{\mathrm{L}} |\mathbf{q}_\ell \cup \mathbf{q}_{\ell-1}|^3 + |\mathbf{q}_0|^3\right)$. Similarly, this expression can be bounded as $O\left(\sum_{\ell=1}^{\mathrm{L}} |\mathbf{q}_\ell \cup \mathbf{q}_{\ell-1}|^3 + |\mathbf{q}_0|^3\right) \leq O\left(\sum_{\ell=1}^{\mathrm{L}} (n_\ell + n_{\ell-1})^3 + n_0^3\right)$. These two expressions enable us to compare the upper-bounds of the start-up cost of the two methods. In Table 1, we give a comparison between the upper-bounds (upp.) of the start-up cost and the effective (eff.) start-up cost for the implementation in this work, see Table 2. We show that here, the start-up cost of SLA is lower than the start-up cost of SGA. The expression for the upper-bound can thus be used for determining which method will exhibit a lower start-up cost.

Table 1. Comparing the start-up costs.

Supermesh	SGA upp.	SGA eff.	SLA upp.	SLA eff.
0	/	/	528^3	528^3
1	/	/	1155^3	1122^3
2	/	/	1551^3	1518^3
3	/	/	2145^3	2112^3
4	/	/	3234^3	3201^3
5	/	/	4422^3	4389^3
6	/	/	6567^3	6567^3
Total	11880^3	11715^3	7481.65^3	7459.21^3

4 MODEL PROBLEM

The model problem we consider for benchmarking the p-MLQMC method, consists of a slope stability problem where the cohesion of the soil has a spatially varying uncertainty, see Whenham et al. (2007). In a slope stability problem, the safety of the slope can be assessed by evaluating the vertical displacement of the top of the slope when sustaining its own weight. We consider the displacement in the plastic domain, which is governed by the Drucker–Prager yield criterion. A small amount of isotropic linear hardening is taken into account for numerical stability reasons. Because of the nonlinear stress-strain relation arising in the plastic domain, a Newton–Raphson iterative solver is used. In order to compute the displacement in a slope stability problem, an incremental load approach is used, i.e., the total load resulting from the weight of

Table 2. Characteristics of the mesh hierarchy for p-MLQMC.

	p-MLQMC			
Level	Nel	DOF	Order	Nquad
0	33	160	2	16
1	33	338	3	19
2	33	582	4	28
3	33	892	5	37
4	33	1268	6	61
5	33	1710	7	73
6	33	2218	8	126

the slope is added in steps starting with a force of 0 N, until the downward force resulting from its weight is reached. This approach results in the following system of equations for the displacement,

$$\mathbf{K}\Delta\mathbf{u} = \mathbf{f} + \Delta\mathbf{f} - \mathbf{k}, \tag{13}$$

where $\Delta\mathbf{u}$ stands for the displacement increment, $\mathbf{K}$ the global stiffness matrix resulting from the assembly of element stiffness matrices $\mathbf{K}^{\mathbf{e}}$, see Eq. (12). The right hand side of Eq. (13) stands for the residual. Here, $\mathbf{f}$ is the sum of the external force increments applied in the previous steps, $\Delta\mathbf{f}$ is the applied load increment of the current step, and $\mathbf{k}$ is the internal force resulting from the stresses. For a more thorough explanation on the methods used to solve the slope stability problem we refer to (de Borst et al., 2012, Chapter 2 §4 and Chapter 7 §3 and §4).

In Table 2 we list the number of elements (Nel), degrees of freedom (DOF), element order (Order), and the number of quadrature points per element (Nquad), per level for the p-MLQMC method. The number of quadrature points in the p-MLQMC method is chosen as to increase the spatial resolution of the field per increasing level, and to ensure numerical stability of the computations of the displacement in the plastic domain. In this paper we consider two-dimensional uniform, Lagrange triangular elements.

The quantity of interest (QoI) is taken as the vertical displacement in meters of the upper left node of the model. This is depicted in Figure 1 by ■. The uncertainty of the cohesion of the soil is represented by means of a log-normal random field. This field is obtained by applying the exponential to the field obtained in Eq. (11), $Z_{\text{lognormal}}(\mathbf{x},\omega) = \exp(Z(\mathbf{x},\omega))$. For the covariance Kernel $C(\mathbf{x},\mathbf{y})$ of the random field, we use the Matérn covariance kernel,

$$\frac{\sigma^2}{2^{\nu-1}\Gamma(\nu)}\left(\sqrt{2\nu}\frac{\|\mathbf{x}-\mathbf{y}\|_2}{\lambda}\right)^{\nu} K_\nu\left(\sqrt{2\nu}\frac{\|\mathbf{x}-\mathbf{y}\|_2}{\lambda}\right), \tag{14}$$

with $\nu = 2.0$ the smoothness parameter, K_ν the modified Bessel function of the second kind, $\sigma^2 = 1$ the variance and $\lambda = 0.2$ the correlation length. The characteristics of the lognormal distribution used to represent the uncertainty of the cohesion of the soil are as follows: a mean of 8.02 kPa and a standard deviation of 400 Pa. The spatial dimensions of the slope are: a length of 20 m, a height of 14 m and a slope angle of 30°. The material characteristics are: a Young's modulus of 30 MPa, a Poisson ratio of 0.25, a density of 1330 kg/m^3 and a friction angle of 20°. Plane strain is considered for this problem. The number of stochastic dimensions considered for the generation of the Gaussian random field is $s = 400$, see Eq. (11). With a value $s = 400$, 99% of the variability of the random field is accounted for.

The stochastic part of our simulations was performed with the Julia packages **MultilevelEstimators.jl**, see Robbe (2018), and **GaussianRandomFields.jl**, see Robbe (2017). The FE code used, is an in-house MATLAB code developed by the Structural Mechanics Section of the KU Leuven, see François et al. (2021). All the results have been computed on a workstation equipped with 2 physical cores, Intel Xeon E5-2680 v3 CPU's, each with 12 logical cores, clocked at 2.50 GHz, and a total of 128 GB RAM.

5 RESULTS

In this section we will discuss the results obtained with the p-MLQMC method. The p-MLQMC method is combined with the improved approaches used to incorporate the uncertainty, i.e., SGA and SLA, as well as the previous approaches, i.e., NNA and LNA. We also compare SGA and SLA against h-ML(Q)MC in terms of computational cost.

ICOSSAR 2021
The 13th International Conference on Structural Safety and Reliability (ICOSSAR 2021), June 21-25, 2021, Shanghai, P.R. China
J. Li, Pol D. Spanos, J.B. Chen & Y.B. Peng (Eds)

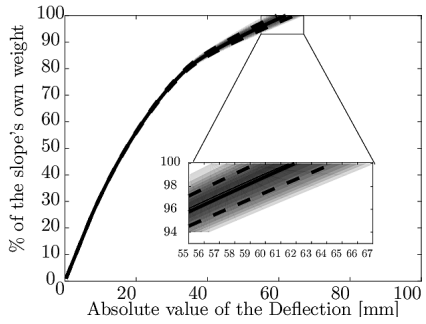

Figure 6. Uncertainty on the QoI.

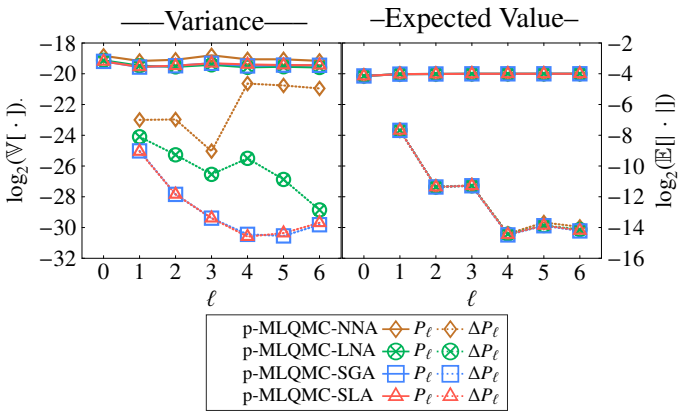

Figure 7. Variance and Expected Value over the levels.

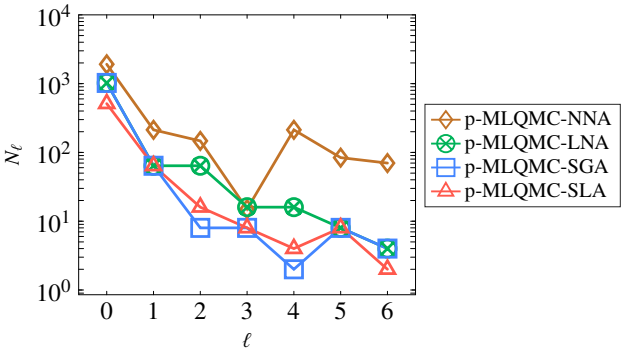

Figure 8. Number of samples per level for a user requested tolerance of 1.165×10^{-5}.

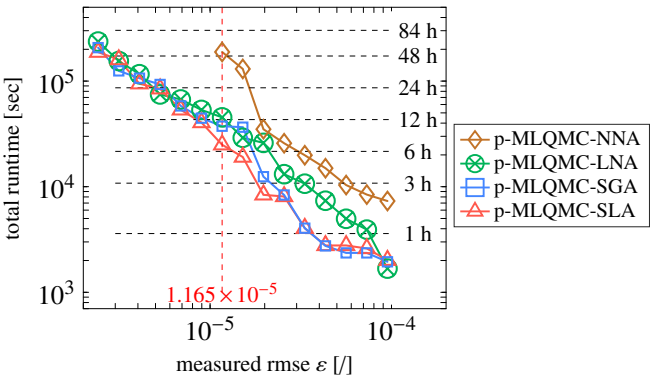

Figure 9. Absolute runtimes in function of the requested user tolerance of NNA, LNA, SGA and SLA.

5.1 *Uncertainty on the QoI*

In Figure 6, we show the uncertainty on the QoI, obtained with the p-MLQMC method. The shades of grey represent the probability density function (PDF), the black line represents the mean, and the black dotted lines represent the 1 sigma bounds.

5.2 *Variance and Expected Value*

In Figure 7, we show the approximation of the variance over the levels $\mathbb{V}[P_\ell]$, the approximation of the variance of the difference over the levels $\mathbb{V}[\Delta P_\ell]$, the approximation of the expected value over the levels $\mathbb{E}[P_\ell]$ and the approximation of the expected value of the difference over the levels $\mathbb{E}[\Delta P_\ell]$.

We observe that $\mathbb{E}[P_\ell]$ remains constant over the levels, while $\mathbb{E}[\Delta P_\ell]$ decreases with increasing level. As explained in §2.4, multilevel methods are based on a variance reduction by means of a hierarchical refinement of FE meshes. In practice this means that the sample variance $\mathbb{V}[P_\ell]$ remains constant across the levels, while the sample variance of the difference over the levels $\mathbb{V}[\Delta P_\ell]$ decreases for increasing level. This is indeed what we observe for LNA, SGA and SLA. For NNA we observe that $\mathbb{V}[\Delta P_\ell]$ does not decrease.

5.3 *Number of samples*

We show the number of samples per level for a user requested tolerance of 1.165×10^{-5} in Figure 8. The corresponding runtime has been indicated in Figure 9 by the vertical line. As expected, the trends of the sample sizes over the levels reflect the trends of the variance of the difference from Figure 7. Except for NNA, all methods show a good decrease of the number of samples per increasing level.

5.4 *Computational complexity*

We show the total runtime as a function of the user-requested tolerance ε on the RMSE in Figure 9.

We observe that the SGA and SLA implementations both outperform the LNA and NNA implementations in terms of computa-

tional cost. LNA is outperformed by a factor ranging between 1 and 3. However, for finer tolerances, the computational cost of LNA, SGA and SLA is equal. This is because for these three approaches, the samples have a strong correlation, see §, 2.4. While LNA has the same cost complexity for finer tolerances, a bias is present on the computed expected value in the telescoping sum. NNA is outperformed by a factor ranging between 4 and 8. The SGA and SLA implementations have the same computational cost for a given tolerance.

5.4.1 *Comparison with h-ML(Q)MC*

In this section we compare the supermesh based approaches combined with the p-MLQMC method against the existing h-ML(Q)MC methods in terms of computational cost. In Fig. 10 we show the computational cost, expressed in seconds for the different approaches used for p-MLQMC, and for h-ML(Q)MC.

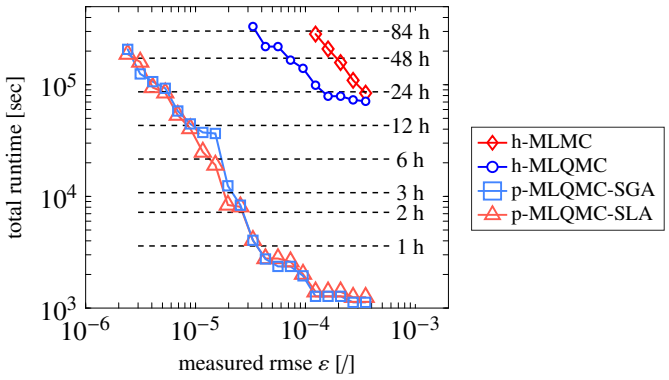

Figure 10. Absolute runtimes in function of the requested user tolerance of SGA, SLA and h-ML(Q)MC.

As can be observed, h-MLQMC is outperformed by a factor 80 by both SGA and SLA, while h-MLMC is outperformed up to a factor 240 by both SGA and SLA.

6 CONCLUSION

In this work we presented two novel approaches based on the integration point method in order to account for the uncertainty in the FE model when a stochastic simulation is performed using p-refined Multilevel quasi-Monte Carlo. These two novels approaches are the Supermesh Global Approach (SGA) and the Supermesh Local Approach (SLA). We have shown at which discrete points the uncertainty, represented as a random field by means of the Karhunen–Loève expansion, is evaluated. We also discussed how to incorporate said uncertainty in the FE model. In addition, we investigated if the telescoping sum remains unbiased when applying either of both methods. We have demonstrated that this is indeed the case. We showed that SGA and SLA both outperform NNA and LNA by a factor 1 to 3, and 4 to 8 respectively. For finer tolerances, the computational cost of LNA is equal to the one of SGA and SLA. The computational cost for SGA and SLA is the same for a given tolerance. Furthermore, we also compared the supermesh approaches against the existing h-MLQMC and h-MLMC methods. We found that SGA and SLA outperform h-MLMC by a factor 240, while h-MLMC is outperformed by a factor 240 by SGA and SLA.

ACKNOWLEDGMENTS

The authors gratefully acknowledge the support from the Research Council of KU Leuven through project C16/17/008 “Efficient methods for large-scale PDE-constrained optimization in the presence of uncertainty and complex technological constraints”. The computational resources and services used in this work were provided by the VSC (Flemish Supercomputer Center), funded by the Research Foundation - Flanders (FWO) and the Flemish Government – department EWI.

REFERENCES

Blondeel, P., Robbe, P., Van hoorickx, C., François, S., Lombaert, G., and Vandewalle, S. (2020). “p-refined multilevel quasi-monte carlo for galerkin finite element methods with applications in civil engineering.” *Algorithms*, 13(5).

Blondeel, P., Robbe, P., Van hoorickx, C., François, S., Lombaert, G., and Vandewalle, S. (2021). “On the selection of random field evaluation points in the p-mlqmc method.” *Accepted for the proceedings of the 14th International Conference in Monte Carlo & Quasi-Monte Carlo Methods in Scientific Computing (MCQMC2020), Oxford, United Kingdom.*

Blondeel, P., Robbe, P., Van hoorickx, C., Lom-

baert, G., and Vandewalle, S. (2018). "The Multilevel Monte Carlo method applied to structural engineering problems with uncertainty in the young's modulus." *Proceedings of the 28th edition of the Biennial ISMA conference on Noise and Vibration Engineering, ISMA 2018*, Desmet, W and Pluymers, B and Moens, D and Rottiers, W (eds), 4899–4913.

Blondeel, P., Robbe, P., Van hoorickx, C., Lombaert, G., and Vandewalle, S. (2019). "Multilevel sampling with Monte Carlo and Quasi-Monte Carlo methods for uncertainty quantification in structural engineering." *Published at the 13th International Conference on Applications of Statistics and Probability in Civil Engineering, ICASP13, Seoul, South Korea.*

de Borst, R., Crisfield, M. A., and Remmers, J. J. C. (2012). *Non Linear Finite Element Analysis of Solids and Structures*. Wiley, U.K.

François, S., Schevenels, M., Dooms, D., Jansen, M., Wambacq, J., Lombaert, G., Degrande, G., and De Roeck, G. (2021). "Stabil: An educational matlab toolbox for static and dynamic structural analysis." *Computer Applications in Engineering Education*, 29(5), 1372–1389.

Giles, M. B. (2008). "Multilevel Monte Carlo path simulation." *Oper. Res.*, 56(3), 607–617.

Giles, M. B. (2015). "Multilevel Monte Carlo methods." *Acta Num.*, 24, 259–328.

Giles, M. B. and Waterhouse, B. J. (2009). "Multilevel Quasi-Monte Carlo path simulation." *Rad. Ser. Comp. App.*, 8, 1–18.

Kuo, F. (2007). "Lattice rule generating vectors. Online `https://web.maths.unsw.edu.au/~fkuo/lattice/index.html` and `https://web.maths.unsw.edu.au/~fkuo/lattice/lattice-32001-1024-1048576.3600`, accessed on 12/04/2019.

Matthies, H. G., Brenner, C. E., Bucher, C. G., and Guedes Soares, C. (1997). "Uncertainties in probabilistic numerical analysis of structures and solids-stochastic finite elements." *Struct. Saf.*, 19(3), 283–336.

Robbe, P. (2017). "Gaussianrandomfields.jl. Online `https://github.com/PieterjanRobbe/GaussianRandomFields.jl`, accessed on 05/11/2020.

Robbe, P. (2018). "Multilevelestimators.jl. Online `https://github.com/PieterjanRobbe/MultilevelEstimators.jl`, accessed on 05/11/2020.

Whenham, V., De Vos, M., Legrand, C., Charlier, R., Maertens, J., and Verbrugge, J.-C. (2007). "Influence of soil suction on trench stability." *Experimental Unsaturated Soil Mechanics*, T. Schanz, ed., Berlin, Heidelberg, Springer Berlin Heidelberg, 495–501.